Investigating the Properties of Higher-Generation Black-Hole Mergers

Meredith Vogel,[1] Matthew Mould,[2] and Davide Gerosa[2]

[1] *University of Florida*

[2] *School of Physics and Astronomy & Institute for Gravitational Wave Astronomy, University of Birmingham, Birmingham, B15 2TT, United Kingdom*

(Dated: August 18, 2021)

In this research we investigate further the fixed point convergence of black hole remnant mass retained and remnant spin magnitude for higher generation mergers done by Gálvez Ghersi and Stein [1]. We use the NRSur7dq4Remnant surrogate model to predict the properties of a population of merging binary black hole remnants via the surfinBH[a] Python package. Many combinations of different initial distribution relationships in black hole mass and spin magnitude such as power, uniform, Gaussian, and delta functions were used to test the fixed point convergences. We find that aligning the spins –meaning the spins were pointed along the orbital angular momentum in each binary direction– changes the fixed point convergences in remnant mass retained, remnant spin magnitude, and kick velocity.

I. INTRODUCTION

Black holes (BHs) form when a star much more massive than the size of our Sun collapses. Binary black holes (BBHs) can come from stellar binaries or from two separate BHs coming together via dynamical processes. In General Relativity (GR) the orbital radius of a BBH system is not constant like in Newtonian gravity. Einstein predicted gravitational waves (GWs) from his general theory of relativity. The mathematics showed that massive accelerating objects like BHs and neutron stars (NSs) would disrupt space time. This disruption would cause a wave to propagate in every direction at the speed of light and it holds information of the origin of the wave. The energy carried away by GWs causes the separation of the objects to shrink, which then causes the objects to merge. This mechanism can cause the mergers of different types of compact-object binaries, e.g., BH-BH, NS-NS, and, as observed very recently [2], BH-NS systems.

These different binaries emit GWs and the most common detections are from BBHs [3]. The first detection was made by LIGO in 2015 named GW150914 [4]. The first NS binary was detected in 2017 by the Advanced LIGO and Advanced Virgo gravitational-wave detectors named GW170817 [5]. Using laser interferometers like LIGO and Virgo, we are able to detect the near end of the binary inspiral. Instead of seeing the Universe with only light, we are now open to a new gravitational perspective.

When two compact objects merge, the result is a single compact remnant. Since LIGO and Virgo have detected BBH mergers, there are BH remnants leftover from their mergers. The first generation of BHs, formed as supernova remnants, therefore produce so-called second-generation BHs. It is important to note that these remnants may be a higher generation if the parents were themselves the products of previous mergers, and there is also the possibility of a merger of mixed generations of BHs.

In this work, we go beyond the mergers of individual BBHs to predict the properties of *populations* of higher-generation BH mergers. Using numerical relativity (NR) surrogate models [6, 7], we estimate the properties of BH mergers and retain the remnant masses and spin magnitudes to construct higher-generation populations. We show that, for various first-generation BH mass and spin distributions, repeated mergers map the population properties of BH remnants to a convergent distribution, as first shown in Ref. [1]. Furthermore, while this remnant distribution is invariant with respect to the initial BH distributions, we show that it does depend on the remnant spins; varying assumptions on the post-merger spin directions can break the original convergence, leading to a different fixed-point remnant distribution at higher generations.

In Section II, we summarize how the properties of BH mergers are estimated by NR surrogate models. In Section III, we describe our method of producing populations of higher-generation BHs. In Section IV we discuss the results of the various simulations performed. In Section V we summarize the work done and talk about what can be done next with this research.

II. MODELING BLACK HOLE BINARY MERGERS

A BH is described by its mass, spin, and charge. The Universe is neutral when looked at in its entirety, therefore astrophysical BHs can be looked at as with neutral charge. It is possible to solve Einstein's GR equations for a single BH, but BBHs are much harder to solve for and do not have exact solutions. A collision of BBHs leaves a remnant which has mass and spin. The remnant also has kick velocity that is in the opposite direction of the GWs. These three properties depend on the two parent BHs. NR is needed to be able to predict these properties accurately. A single BBH NR simulation can take months to do on a supercomputer. Instead, we use NR surrogate models [6, 7].

[a] pypi.org/project/surfinBH/

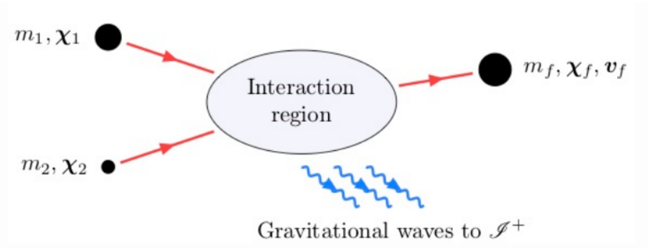

FIG. 1. The surrogate model, which is fit to NR simulations, approximates the merger of two BHs. The input parameters are the mass m_1 (m_2) and dimensionless spin vectors $\boldsymbol{\chi}_1$ ($\boldsymbol{\chi}_2$) of the primary (secondary) BH. The surrogate outputs the mass m_f, dimensionless spin vector $\boldsymbol{\chi}_f$ and recoil velocity vector $\boldsymbol{v}_f$ of the remnant BH. Figure taken from Ref. [6].

This surrogate model is a fit to NR simulations that have already been done. They are much quicker to evaluate, taking ~ 1 second on an off-the-shelf personal computer. They are also still very accurate, as long as they are used in the region of parameter space they have been trained in. Surrogate models can be trained for any BH mass or spin and the accuracy correlates with the NR simulations. Figure 1 is a visual representation of the surrogate model. [6, 7].

Binaries that have misaligned spins with respect to the orbital angular momentum are complicated to model analytically. The spins of the binary interact with the orbital angular momentum and each other; therefore the system precesses about the direction of the total angular momentum. Precession appears as characteristic modulations in amplitude and frequency of GWs. For nonprecessing systems, the direction of the orbital angular momentum $\mathbf{L}$ is fixed, e.g., along the z direction. Gravitational radiation is the strongest along directions that are parallel and antiparallel to $\mathbf{L}$. For precessing systems, the direction of $\mathbf{L}$ varies, so there is not a fixed axis where radiation is dominant. The BHs are always along the x axis, with the heavier of the two on the positive x axis. This is called the co-orbital frame and it is non-oscillatory which simplifies the description of the dynamics.

The surrogate models are parameterized by mass ratio $q = m_1/m_2 \geqslant 1$ and two spin vectors $\boldsymbol{\chi}_{1,2}$, where the index 1 labels the larger BH and 2 the smaller. We use the NRSur7dq4 model, which was trained against 1528 precessing NR simulations with mass ratios $q \leq 4$, spin magnitudes $\chi_{1,2} = |\boldsymbol{\chi}_{1,2}| \leq 0.8$, and with generic spin directions [7]. The mass ratio q can be extrapolated to ≤ 6 and spin magnitudes up to $\chi_{1,2} \leqslant 1$ and the accuracy is still comparable or better than existing models, but still must be used with caution. From input inputs values for q and the spin vectors $\boldsymbol{\chi}_{1,2}$ in the co-orbital frame at a reference time during the inspiral, the surrogate will output the predicted remnant mass m_f, remnant spin vector $\boldsymbol{\chi}_f$, and the kick velocity $\boldsymbol{v}_f$ [7] (with remnant vectors defined with respect to the same pre-merger frame). Above and in the following, we use geometric units in which $G = c = 1$.

III. METHOD

The NR surrogate predicts single BH remnant properties, while here, we study populations of merger products produced from seed BH distributions. Gálvez Ghersi and Stein [1] found the distributions of remnant spin magnitude and fractional mass loss evolved to a fixed point distribution that converged in about five to six merger generations. These convergences did not depend on initial conditions. Following their approach, we investigate in more detail the convergence of remnant BH distributions. We use the NRSur7dq4Remnant surrogate model to predict the properties of merging BBHs via the surfinBH[1] Python package.

For each simulation, 10^4 BHs were sampled with masses from an initial distribution in the range $[8, 48]M_\odot$ (which enforces $q \leqslant 6$) and spin magnitudes up to 0.8. We considered several different distributions in both mass and spin –uniform, power law, Gaussian, and delta distributions– and described in this paper are the cases of uniform and delta distributions. We then randomly sampled (with repetition) 10^4 BH pairs from the initial distributions in mass and spin to form a population of merging binaries. The properties of each merger remnant was estimated with the surrogate model. The remnant parameter distributions then become the initial conditions for the next generation of BHs, and so on for n generations; we take $n = 20$ generations. Therefore, it is possible to study how the mass and spin distributions change per generation.

While the surrogate predicts not only the remnant spin magnitude but also the spin direction, we retain the magnitude of each remnant BH for the next generation but resample the spin direction. We consider two cases. Firstly, at each generation the spin directions are resampled isotropically; this models the redistribution of spins via repeated interactions in a dynamical environment. Secondly, we form a mixed population of isotropically resmapled spins and spins aligned with the binary orbital angular momentum; this models a subpopulation of BBHs whose spins are subject to an alignment mechanism within a dynamical environment, such as the disks of active galactic nuclei. In the isotropic and aligned spin case, at each generation, 20% of the spin directions were isotropic and 80% of the spin directions were aligned. The kick velocity can remove the remnant BH from its host environment, but this is ignored here since we are only interested in parameter distributions.

By varying the various assumptions in this model, e.g., the initial BH distributions and the spin resampling, we aim to investigate the robustness of the convergence to fixed-point remnant distributions found in Ref. [1].

[1] pypi.org/project/surfinBH/

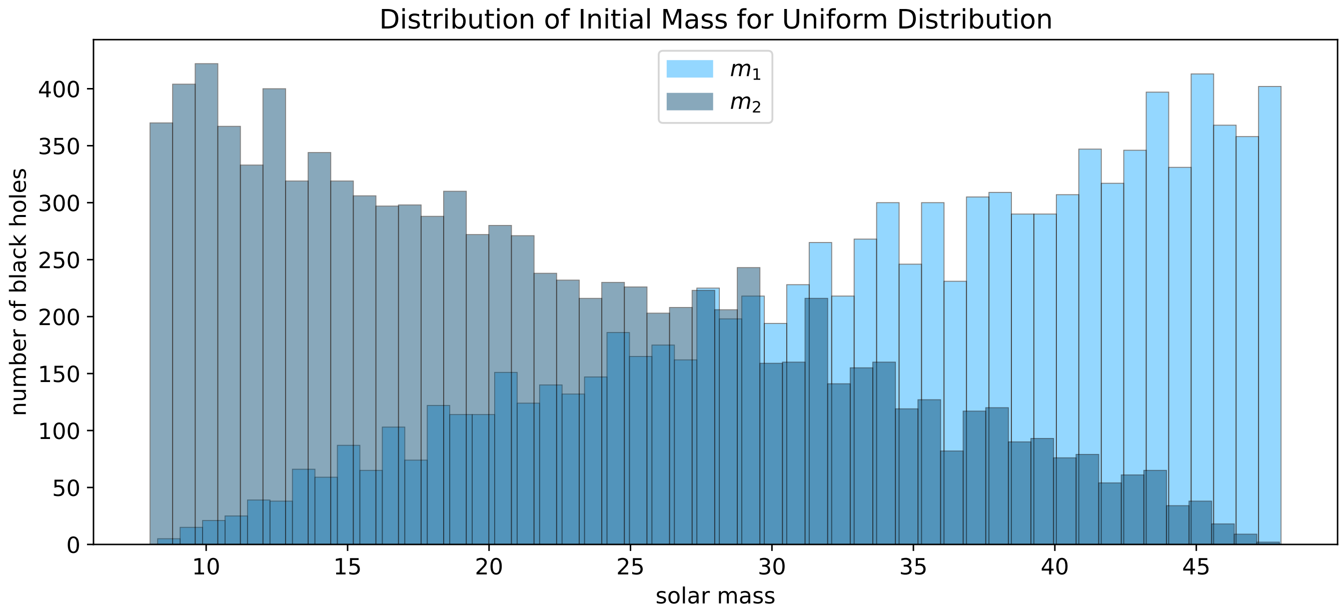

FIG. 2. The initial mass distribution for a uniform distribution. The parameters plotted, m_1 and m_2, are the masses of the merging BHs.

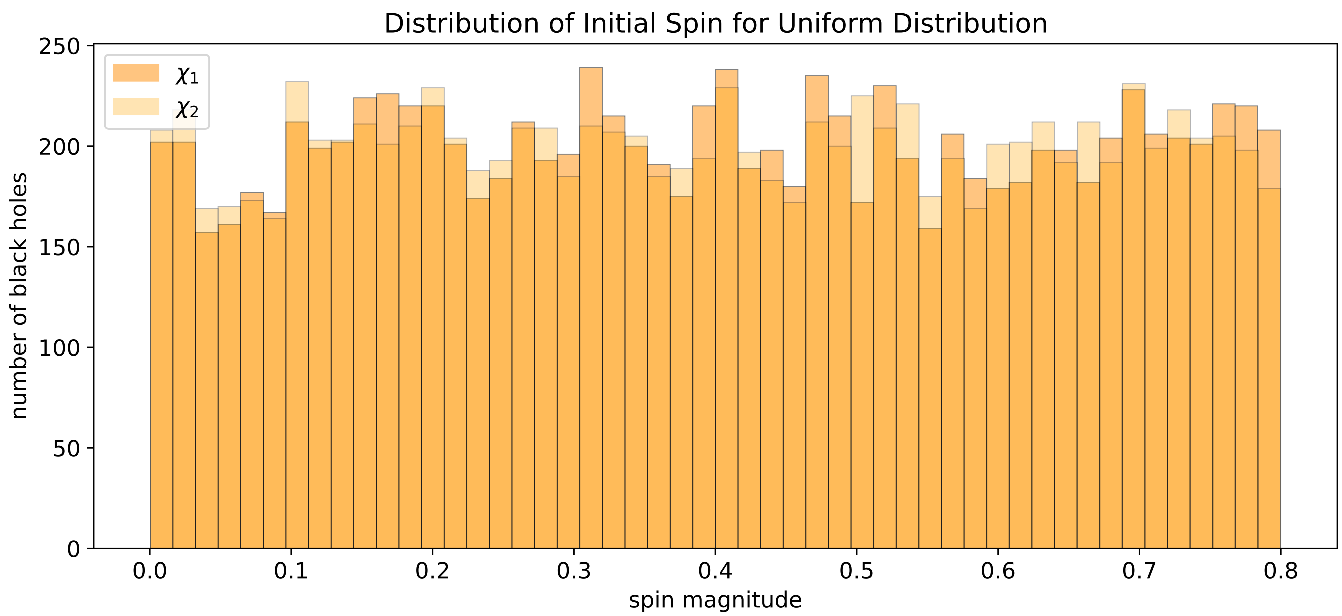

FIG. 3. The initial spin distribution for a uniform distribution. The parameters plotted, χ_1 and χ_2, are the spin magnitudes of the merging BHs.

IV. RESULTS

In the first column of the corner plots in this paper is

$$\mu_{\rm rel} \coloneqq \frac{m_f}{m_1 + m_2}\,, \tag{1}$$

which is the fraction of mass retained after the merger; the rest of the mass is radiated via GWs. In the second column is χ_f which is the remnant spin magnitude and in the third column is v_f or the remnant kick magnitude in terms of the speed of light. At top of each column are the one-dimensional marginal distributions for $\mu_{\rm rel}$, χ_f, and v_f. The plot in the first column and second row is the two-dimensional relationship between χ_f and $\mu_{\rm rel}$, and so on for the other two plots. In each case we plot the 12%, 39%, 68% and 86% contour levels. Notice in the surrogate

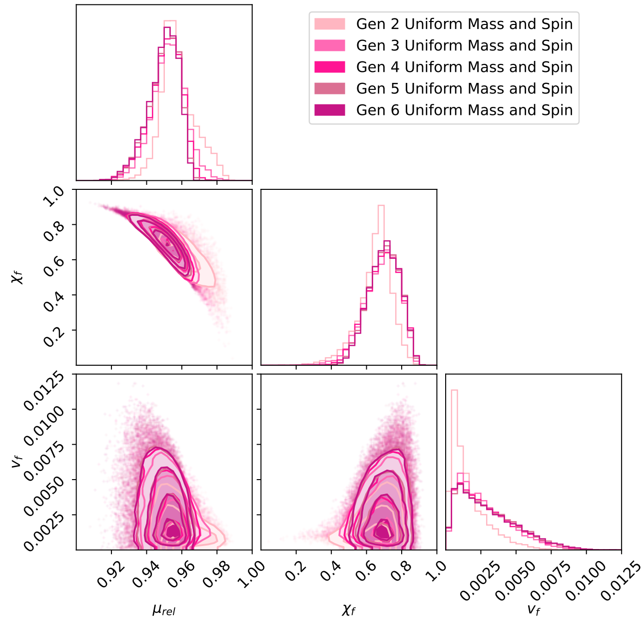

FIG. 4. Remnant mass retained (μ_{rel}), spin magnitude (χ_f), and kick velocity (v_f) in terms of c for generations two through six. Initial BH masses and spins were both chosen from uniform distributions. The darker the color, the higher the generation.

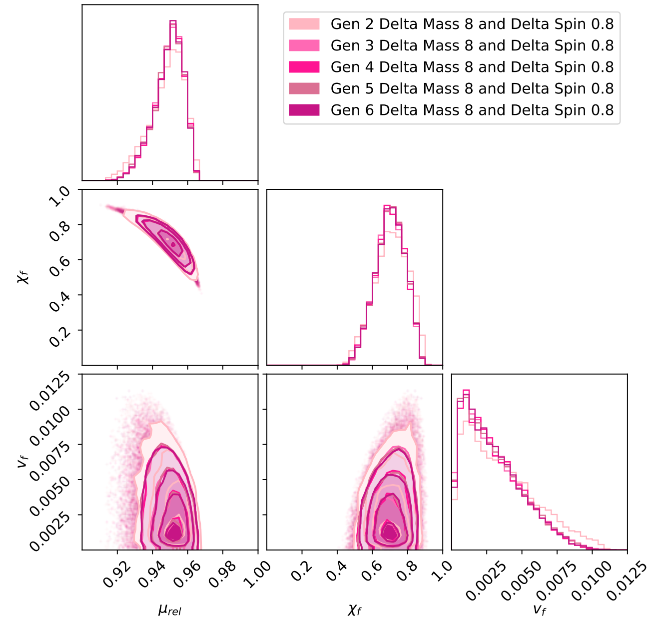

FIG. 5. Remnant mass retained (μ_{rel}), spin magnitude (χ_f), and kick velocity (v_f) in terms of c for generations two through six. BBH mass picked from a delta function of eight solar masses and spin picked from a delta function of 0.8. The darker the color, the higher the generation.

model diagram, the output is m_f, the remnant mass, but for plotting we use the fraction of the mass retained after the merger $\mu_{\rm rel}$.

A. Uniform black hole distributions

The first case is for an initial BH distribution that is uniform in mass and spin, as illustrated in Figs. 2 and 3. A BH was sampled randomly from the distribution described above and paired with a second BH chosen the same way, while enforcing $m_1 \geqslant m_2$.

In Fig. 4, we plot the remnant BH distributions over several merger generations for this first case. The mass retained and spin magnitude start to converge right away and distinguishing generations becomes difficult after the fourth generation for the mass and the third generation for the spin magnitude. Figure 4 also shows that all of the one- and two-dimensional distributions converge to a fixed-point, including the kick velocity (cf. Fig. 10 of Ref. [1]).

B. Delta distributions

A more restrictive case is a delta function in initial mass and spin plotted in Fig. 5. Here, the initial BH masses are all taken to be $8M_\odot$ and the initial spin magnitudes are 0.8. The delta relationship with the initial distributions caused convergence earlier than any other case since the initial distribution was the same value for every BH. The distributions begin to become indistinguishable immediately at the second generation for mass, spin and kick.

We verified these results hold for many different combinations of delta functions in mass and spin. Different delta functions are essentially different magnitudes of each other, so their distributions will look very similar to each other.

C. Mixed isotropic and aligned spin resampling

We also explored the effect of resampling the post-merger spin directions with a mixture of aligned and isotropic BH spins, with various cases where $x\%$ of the spins were isotropic and $100 - x\%$ aligned. Figure 6 illustrates the particular simulation for 20% isotropic spins and 80% aligned spins, meaning most of the spins were pointed along the orbital angular momentum in each binary.

Spin alignment broke the convergence of the remnant parameters; the spin magnitude and retained remnant mass distribution changed in comparison to the other cases, but still converged to a fixed point. The mass retained converges later than the spin magnitude does for the aligned spins case. The generations converge at the fourth generation for mass and in the second or third for the spin magnitude. The combination of the two spin-direction distributions also leads to two apparent components in the two-dimensional kick distributions –

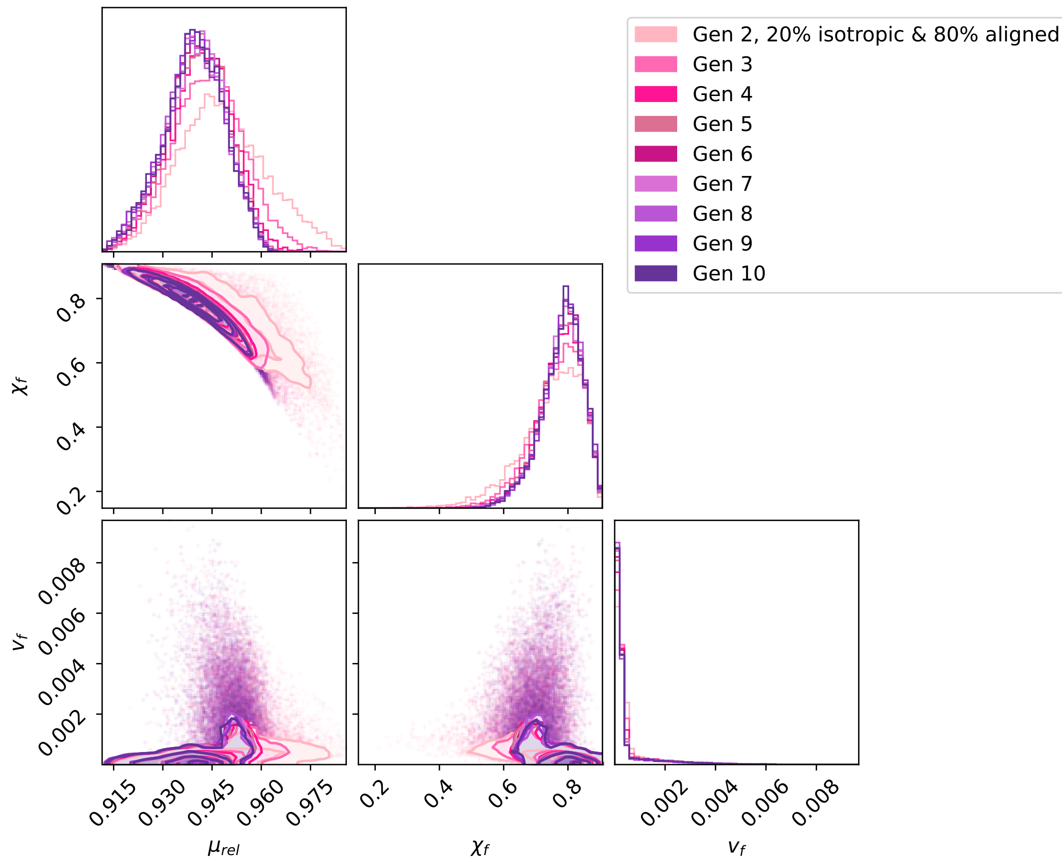

FIG. 6. Remnant mass retained (μ_{rel}), spin magnitude (χ_f), and kick velocity (v_f) in terms of c for generations one through ten. The BH spins were sampled with 20% isotropic and 80% aligned at each merger generation. The darker the color, the higher the generation.

a larger and broader component from the majority 80% aligned-spin merger, and a smaller component from the 20% of binaries with isotropically distributed spins. Since the recoil velocity is sensitive to the pre-merger spin orientations, the one-dimensional kick distribution is much narrower compared to the previous cases due to the more restrictive assumption of spin alignment.

D. Comparison of cases

When a power, Gaussian, delta, or uniform distribution in mass or spin was used, the remnant BH properties converged to about the same fixed point. Figure 7 shows a comparison of the convergences when using uniform and delta distributions in initial masses and spin magnitudes, and the aligned vs. isotropic spins case. The mass converges to $\sim 95\%$ mass retained for the uniform and delta distributions. The remnant spin magnitude converges to ~ 0.7 and does not go below ~ 0.4. This spin magnitude has previously been observed using astrophysical environments and semi-analytic modeling [8, 9]. This value is also a conversion of the orbital angular momentum of the binary to the spin angular momentum of the remnant [1].

The total remnant mass distribution becomes more narrow as the number of generations increases because of the loss of memory of the initial mass distribution. The second generation and fourth generations are plotted to show the convergence and because the fourth generation is the latest the cases had converged by for both mass and spin.

The case where the spins are aligned 80% of the time is where the convergence in spin magnitude and mass retained changes. The mass retained decreases, peaking at $\sim 94\%$, and is spread over a wider range as the number of generations increases. The spin magnitude is higher than the other cases, now peaking at ~ 0.8, and spread over a smaller range of about 0.6 to $\lesssim 1.0$. This makes sense because if the spins are aligned, they are in the same direction, and they add together for the remnant spin magnitude. Therefore, the spin magnitude of a remnant whose parents had aligned spins will have a high spin magnitude. Lastly, the kick velocity is in a tight distribution and is slower (in terms of c) than the other cases. Investigating the spins or spin directions of the BH mergers may continue to show discrepancies in the convergence of remnant mass retained and remnant spin magnitude.

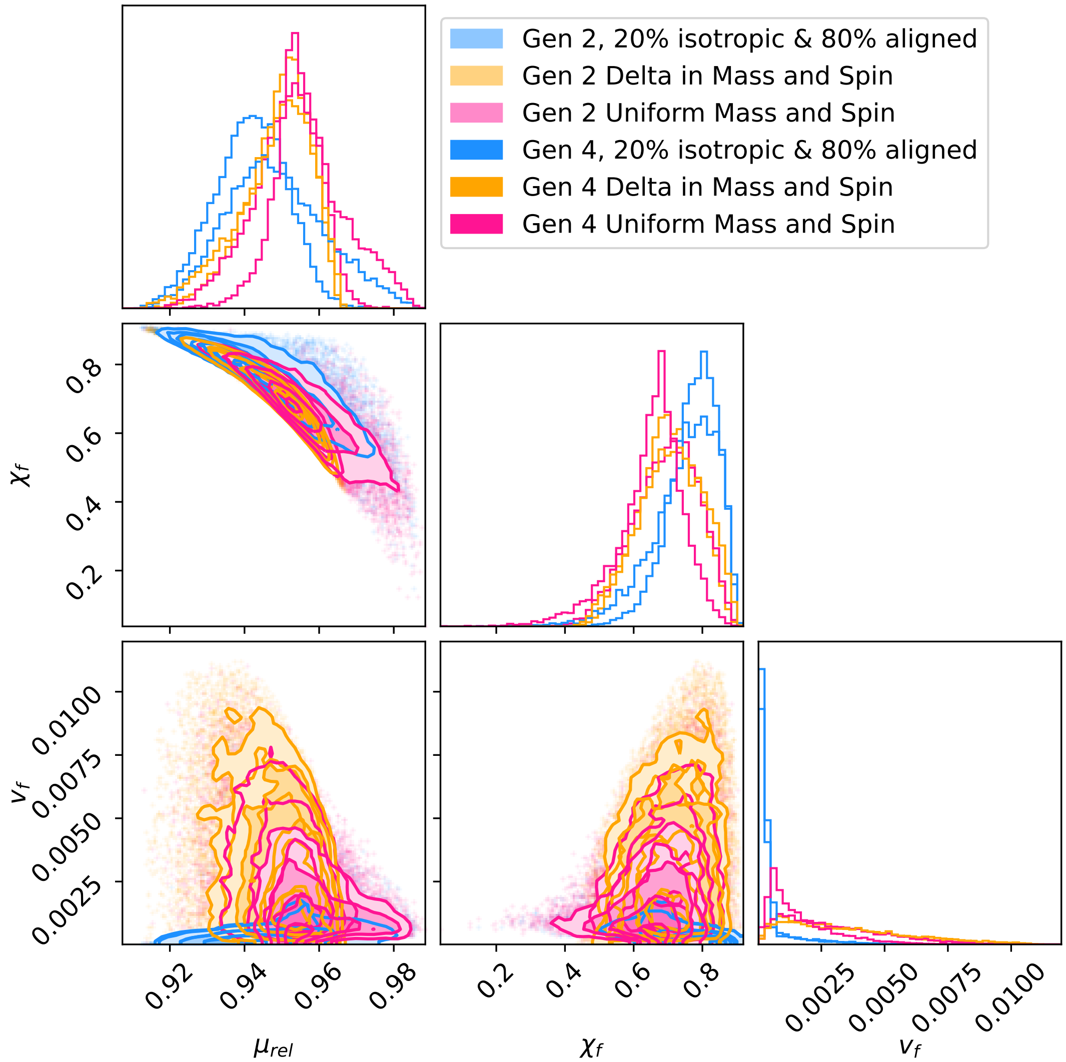

FIG. 7. All three cases (uniform mass and spin, delta mass and spin, and uniform mass and isotropic and aligned spin) are plotted for the second and fourth generations.

V. CONCLUSIONS AND FUTURE WORK

We investigated the convergence of BH remnant properties from higher generation mergers. We used NRSur7dq4Remnant [7], a surrogate model fit to NR simulations, to merge many BBHs for multiple generations accurately and efficiently. We found that using power, Gaussian, delta, or uniform relationships on the initial distribution of BH mass and spin causes the remnant mass retained and spin magnitude to converge to a fixed point like in the work done by Gálvez Ghersi and Stein [1]. We found that when the spins of the BBHs were aligned, the remnant mass retained and spin magnitude convergences changed. More of the remnant mass was radiated away via GWs, the spin magnitude increased, and the kick velocity decreased.

Many other paths can be explored within this project. Instead of randomly pairing BHs, it may be more physical to have selective pairing. BHs are more selective of their pairing with another of similar mass [10]. A second way to add more astrophysics is by investigating how the kick velocity changes the distributions of remnant properties. If the kick velocity is higher than the escape velocity of an environment with multiple BHs, the BH will not continue to merge with the BHs in the group. Then, the kick velocity may have a larger impact on the remnant distributions. Lastly, mixed generational pairing was mentioned in the beginning of this paper and is not included in the work of this research. The events observed by LIGO and Virgo may have been mixed-generation mergers, therefore it is worthwhile to investigate the remnant property distributions of BHs of mixed generation pairings.

ACKNOWLEDGMENTS

I would like to thank Matthew Mould for working one on one with me throughout the summer of 2021 remotely due to COVID-19. He was incredibly patient with teaching gravitational research to someone new to the field and did a phenomenal job teaching the material and methods as well. I want to thank my official mentor Davide Gerosa for welcoming me into his research group and allowing me to research one of the most interesting projects I've done. Thank you to Michela Mapelli for being my host at the University of Padova in Italy. Thank you to the University of Florida International and the National Science Foundation for funding this project and international travel (NSF PHY-1950830 and NSF PHY-1460803). Finally, thank you to Paul Fulda, Peter Wass, and Nathaniel Strauss.

[1] J. T. Gálvez Ghersi and L. C. Stein, Classical and Quantum Gravity **38**, 045012 (2020).

[2] R. Abbott, T. D. Abbott, S. Abraham, F. Acernese, K. Ackley, A. Adams, C. Adams, R. X. Adhikari, V. B. Adya, C. Affeldt, and et al., The Astrophysical Journal Letters **915**, L5 (2021).

[3] R. Abbott, T. Abbott, S. Abraham, F. Acernese, K. Ackley, A. Adams, C. Adams, R. Adhikari, V. Adya, C. Affeldt, and et al., Physical Review X **11**, 10.1103/physrevx.11.021053 (2021).

[4] B. P. Abbott, R. Abbott, T. D. Abbott, M. R. Abernathy, F. Acernese, K. Ackley, C. Adams, T. Adams, P. Addesso, R. X. Adhikari, *et al.* (LIGO Scientific Collaboration and Virgo Collaboration), Phys. Rev. Lett. **116**, 061102 (2016).

[5] B. Abbott, R. Abbott, T. Abbott, F. Acernese, K. Ackley, C. Adams, T. Adams, P. Addesso, R. Adhikari, V. Adya, *et al.*, Physical Review Letters **119**, 10.1103/physrevlett.119.161101 (2017).

[6] V. Varma, D. Gerosa, L. C. Stein, F. Hébert, and H. Zhang, Physical Review Letters **122**, 10.1103/physrevlett.122.011101 (2019).

[7] V. Varma, S. E. Field, M. A. Scheel, J. Blackman, D. Gerosa, L. C. Stein, L. E. Kidder, and H. P. Pfeiffer, Physical Review Research **1**, 10.1103/physrevresearch.1.033015 (2019).

[8] D. Gerosa, S. Vitale, and E. Berti, Physical Review Letters **125**, 10.1103/physrevlett.125.101103 (2020).

[9] M. Fishbach, D. E. Holz, and B. Farr, The Astrophysical Journal **840**, L24 (2017).

[10] M. Fishbach and D. E. Holz, The Astrophysical Journal **891**, L27 (2020).